THE JOURNAL OF PHYSICAL CHEMISTRY Letters

Letter

pubs.acs.org/JPCL

Dissecting Local Atomic and Intermolecular Interactions of Transition-Metal Ions in Solution with Selective X-ray Spectroscopy

Philippe Wernet,*[,†] Kristjan Kunnus,[†,‡] Simon Schreck,[†,‡] Wilson Quevedo,[†] Reshmi Kurian,[§] Simone Techert,[#] Frank M. F. de Groot,[§] Michael Odelius,[∥] and Alexander Föhlisch[†,‡]

[†]Institute for Methods and Instrumentation for Synchrotron Radiation Research, Helmholtz-Zentrum Berlin für Materialien und Energie GmbH, Albert-Einstein-Strasse 15, 12489 Berlin, Germany

[‡]Institut für Physik und Astronomie, Universität Potsdam, Karl-Liebknecht-Strasse 24/25, 14476 Potsdam, Germany

[§]Inorganic Chemistry & Catalysis, Debye Institute for Nanomaterials Science, Utrecht University, Universiteitsweg 99, 3584 CG, The Netherlands

[#]Structural Dynamics of (Bio)chemical Systems, Max Planck Institute for Biophysical Chemistry, 37070 Göttingen, Germany

[∥]Department of Physics, AlbaNova University Center, Stockholm University, 106 91 Stockholm, Sweden

Supporting Information

ABSTRACT: Determining covalent and charge-transfer contributions to bonding in solution has remained an experimental challenge. Here, the quenching of fluorescence decay channels as expressed in dips in the L-edge X-ray spectra of solvated 3d transition-metal ions and complexes was reported as a probe. With a full set of experimental and theoretical ab initio L-edge X-ray spectra of aqueous Cr^{3+}, including resonant inelastic X-ray scattering, we address covalency and charge transfer for this prototypical transition-metal ion in solution. We dissect local atomic effects from intermolecular interactions and quantify X-ray optical effects. We find no evidence for the asserted ultrafast charge transfer to the solvent and show that the dips are readily explained by X-ray optical effects and local atomic state dependence of the fluorescence yield. Instead, we find, besides ionic interactions, a covalent contribution to the bonding in the aqueous complex of ligand-to-metal charge-transfer character.

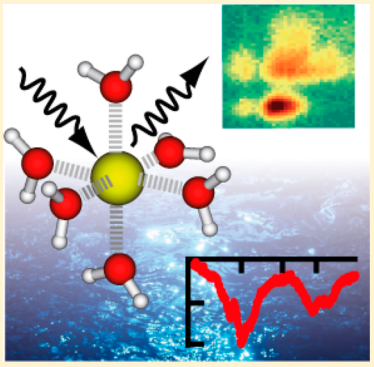

SECTION: Liquids; Chemical and Dynamical Processes in Solution

The transfer of charge from a solvated ion or molecular complex to the surrounding solvent is an elementary step in numerous reactions in nature and in technological processes. Understanding charge transfer to solvent effects in molecular systems is thus of primary importance, and X-ray spectroscopy with its specificity to elemental and chemical sites promises to add a new suite of powerful tools for their investigation.[1] Specifically, time-resolved X-ray spectroscopy[2−11] appears to be the most direct way of probing charge transfer initiated by a pump pulse and probed as a function of time by scanning the delay of a short X-ray probe pulse. However, such effects can proceed on the few-femtosecond time scale, and it is currently very challenging to achieve a corresponding time resolution in pump−probe X-ray spectroscopy experiments. Therefore, it has been attempted to make use of the core−hole lifetime of a few femtoseconds to study ultrafast charge-transfer processes for various systems such as for adsorbates on surfaces,[12−18] ice,[19] and aqueous solutions.[20] Using resonant soft X-ray spectroscopy, a core electron is excited into an unoccupied state of the system, and the probability for it to transfer to the surroundings during the few-femtosecond core−hole lifetime will influence the core−hole decay channels. The Auger decay signal is thus stronger the higher the probability for its transfer to the surrounding medium during the core−hole lifetime.[15,17,18]

As core-excited states can decay via Auger electron ejection or fluorescence, the question arises whether such ultrafast electron-transfer processes are observable in the fluorescence decay channel as well. This relates to the more general questions as to whether and how bonding and charge-transfer processes can be revealed with X-ray spectroscopy. Along these lines, Aziz et al. recently reported the so-called "dark channel fluorescence yield" method.[21,22] They found features in the total fluorescence yield (TFY) spectra when scanning the L-edges of 3d transition-metal ions and complexes in solution at high concentration that dip below the fluorescence background of the solvent. It was claimed that this could be used as a new tool to study charge transfer to solvent effects.[21−24] The dips where attributed, first, to ultrafast electron transfer from the metal d orbitals to the solvent[21−24] and, second, to a competition of solute and solvent fluorescence.[25] Earlier, Näslund et al. proposed strong orbital mixing between the 3d orbitals of Fe ions solvated in water based on an analysis of the O K-edge absorption spectrum of aqueous solutions[26] without making a connection to any charge transfer.

Received: September 21, 2012
Accepted: November 6, 2012

   dx.doi.org/10.1021/jz301486u | J. Phys. Chem. Lett. 2012, 3, 3448−3453

In the context of dark channel fluorescence yield, Aziz et al. interpreted this orbital mixing as supportive for the assertion of ultrafast electron transfer from the metal d orbitals to the solvent as deduced from the metal ion L-edge spectra.[21] This electron transfer would occur during the core−hole lifetime of the core-excited state in the metal ion; as the electron excited upon X-ray absorption would have transferred to the solvent, the corresponding fluorescence decay channel would be quenched, leaving a dip in the metal ion L-edge spectrum.[21−24] It was claimed that the transfer would be the more efficient and, correspondingly, the dip would be the deeper the stronger the orbital overlap between the metal d orbitals and the solvent orbitals. While resonant photoelectron and fluorescence yield spectroscopies of aqueous Co^{2+} ions have been used to allegedly confirm the origin of dark channel fluorescence,[27,28] recent investigations based on calculated spectra of free metal ions[29] and measured spectra of a solid compound[30] proposed alternative explanations for the observed dips.

Here, we address the bonding and possible charge transfer via the dark channel fluorescence yield of ions in aqueous solution. A full set of experimental X-ray data with calculated spectra from ab initio theory enable us to unambiguously disentangle local atomic effects from intermolecular interactions. In addition, we accurately quantify all "X-ray optical effects". We address, in particular, the possible explanation of dips in the TFY metal ion spectra by charge transfer to solvent for the exemplary case of Cr^{3+} ions solvated in water.

The X-ray absorption spectrum of aqueous Cr^{3+} ions as measured in transmission mode is compared in Figure 1 with the TFY spectrum, the O and Cr partial fluorescence yield (PFY) spectra (O and Cr PFY, respectively), and simulated spectra corresponding to the respective detection modes. The O and Cr PFY spectra denote X-ray spectra where, as in all other spectra, the incident photon energy was scanned across the Cr L-edges while the fluorescence from the O K-edge and Cr L-edges was detected, respectively (see the Experimental Section). All simulated spectra (denoted with "Sim." in the figures) were calculated with the standard formula for fluorescence-detected X-ray absorption[29,31] (see the Theoretical Calculations section). They include various X-ray optical effects, such as a variation of the solvent or background fluorescence intensity due to changes in relative solute−solvent absorption strengths when crossing the solute absorption edges and effects due to saturation and self-absorption. The simulations rely on the experimental Cr L-edge (Figure 1a) and O K-edge (not shown) transmission spectra as inputs for solute and solvent absorption cross sections and on experimental Cr L-edge RIXS (Figure 2a) and O K-edge X-ray emission spectra (not shown) to account for the spectral distributions of emitted photons. They do not include any effects on the spectra due to a hypothetical charge transfer to the solvent.

While the transmission-mode spectrum in Figure 1a reflects the true absorption cross section, the TFY spectrum (Figure 1b) can be characterized by dips for all multiplet components at both the L_3- (578 eV) and the L_2-edges (587 eV). The simulated TFY spectrum in Figure 1b reproduces the dips in the measured TFY spectrum, except for a small deviation of the intensities at the L_3-edge. This demonstrates that the dips in the Cr TFY spectrum are largely due to X-ray optical effects. The measured and simulated O PFY spectra in Figure 1c prove, in particular, that they are mainly due to a corresponding variation in the background (solvent O K-edge) fluorescence. The perfect match between measured and simulated O PFY spectra in Figure 1c is

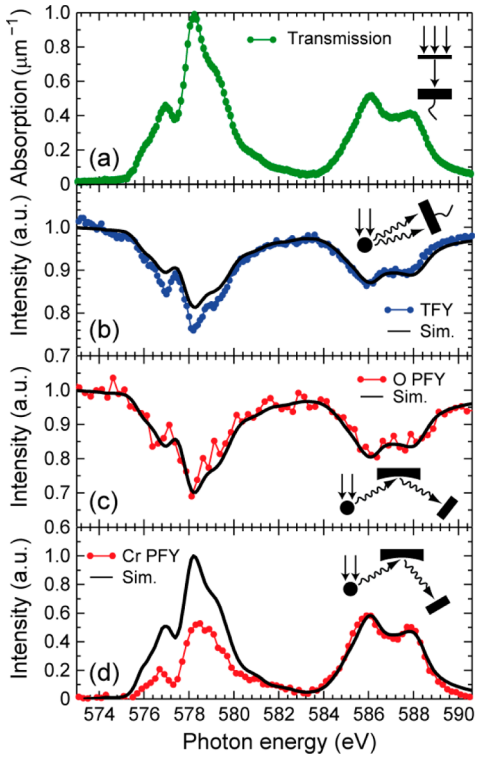

Figure 1. Comparison of experimental and simulated X-ray spectra at the Cr $L_{3,2}$-edges with schematical depictions of the corresponding experimental arrangement in the insets. (a) Experimental X-ray absorption spectrum measured in transmission mode. (b) Measured TFY spectrum (circles) and simulated TFY spectrum (line). (c) Measured PFY spectrum by detecting the oxygen K emission (O PFY spectrum, circles) and simulation of the O PFY spectrum. (d) Measured PFY spectrum by detecting the Cr $L_{3,2}$ emission (Cr PFY spectrum, circles) and simulation of the Cr PFY spectrum with constant fluorescence yield of 3.7×10^{-3}. All spectra are normalized to 1 at the maximum.

furthermore consistent with the finding that it is possible to extract the true absorption spectrum from PFY spectra, as recently shown by Achkar et al.[32] The Cr PFY spectrum in Figure 1d strongly deviates from the absorption cross section (Figure 1a). In contrast to the transmission mode spectrum, L_3- and L_2-edges are approximately equally intense in the Cr PFY spectrum. This is a clear manifestation of state- or incident-photon-energy dependence of the Cr fluorescence yield. This effect was recently predicted by calculations by Kurian et al. (unpublished results) and earlier by calculations in ref 33, and it is detailed below in Figure 2. The simulated Cr PFY spectrum in Figure 1d strongly overestimates the intensity at the L_3-edge compared to the measured spectrum as the simulation is based on a constant fluorescence yield of 3.7×10^{-334} for all states and, in particular, for both edges. The question arises whether the small disagreement of the simulated TFY with experiment at the L_3-edge (Figure 1b) is due to this shortcoming of the simulation with constant fluorescence yield or whether other effects such as charge transfer to solvent are needed to explain it.

Before refining the Cr PFY simulation, we now turn to a short discussion of the state dependence of the Cr fluorescence yield. This is done with the measured resonant inelastic X-ray scattering (RIXS) plane in Figure 2a, where fluorescence intensities at the Cr L-edges are plotted versus the incident photon energy and the energy transfer. In Figure 2b, we plot Cr PFY spectra as extracted for the given energy-transfer ranges.

dx.doi.org/10.1021/jz301486u | J. Phys. Chem. Lett. 2012, 3, 3448−3453

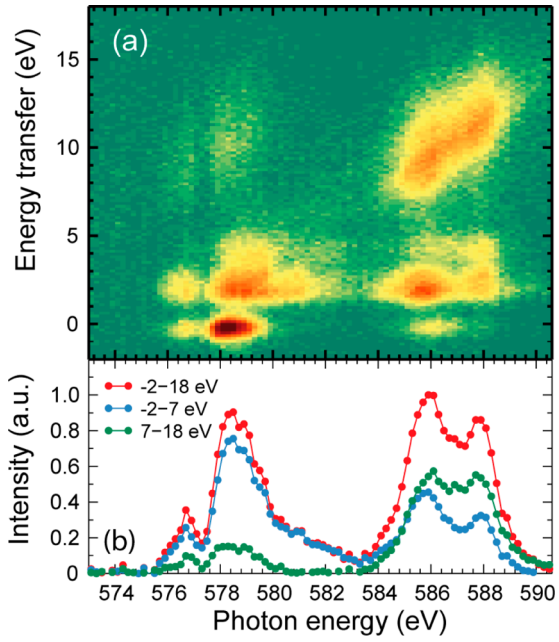

Figure 2. Cr $L_{3,2}$ resonant inelastic X-ray scattering (RIXS) spectra. (a) Full RIXS plane displaying fluorescence intensities in a false-color plot representation with intensities encoded in color (green: small intensity; dark red: large intensity) versus energy transfer (vertical) and incident photon energy (horizontal). (b) Partial fluorescence yield spectra as extracted from (a) for the given energy-transfer regions (circles connected by lines). The spectrum for energy transfers of −2 to 18 eV is the same as that in Figure 1d. It is normalized to 1 at the maximum, and all other spectra are plotted with respective intensities.

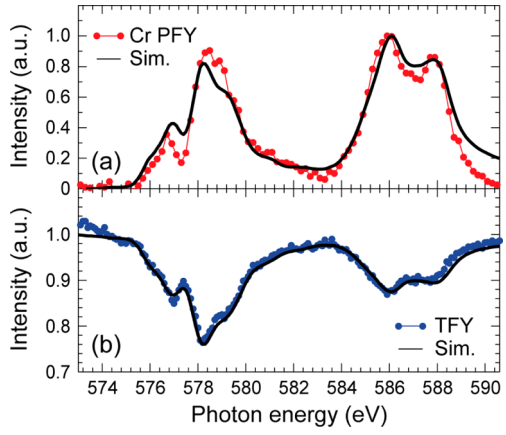

Figure 3. Comparison of experimental and refined simulated X-ray spectra at the Cr $L_{3,2}$-edges. (a) Measured Cr $L_{3,2}$ PFY spectrum (Cr PFY spectrum, circles, same as Figure 1d) and simulation of the Cr PFY spectrum (line) with different fluorescence yields for L_3 (2.0×10^{-3}) and L_2 (3.7×10^{-3}) as obtained from a best fit of the simulated to the experimental data. (b) Measured TFY spectrum (circles) and simulated TFY spectrum (line) with the fluorescence yields for L_3 and L_2 as determined in (a). All spectra are normalized to 1 at the maximum.

The energy transfer is simply defined as the difference between the incident photon energy and the fluorescence or emission energy. The striking feature in the RIXS plane to be noted first is the strong intensity at the L_2-edge and at energy transfers of around 11 eV. This is due to Coster−Kronig (CK) decays[35] of L_2 holes, as can be easily justified by the approximately 9 eV difference to the energy losses of the main fluorescence centered approximately at 2 eV at the L_2-edge and in perfect correspondence with the L_3−L_2 spin−orbit splitting of approximately 9 eV. Such CK signals can be common features in X-ray spectra and have also been recently discussed for Fe^{2+} ions in aqueous solution.[36]

The CK signal observed here does not explain the equal intensity of L_3- and L_2-edges in the PFY spectrum as CK decays reshuffle intensities in the RIXS plane along the vertical (energy-transfer) axis but not between L_3- and L_2-edges. Instead, differences of the fluorescence yields for corresponding energy-transfer regions at the L_3-edge compared to those of the L_2- edge, as is apparent from the RIXS plane in Figure 2a, are responsible for the deviation of the Cr PFY spectrum (transfers of −2 to 18 eV in Figure 2b) from the absorption spectrum. Note, for example, that the fluorescence intensities at or close to zero energy transfer are stronger at the L_3-edge compared to that at the L_2-edge. Instead, the fluorescence is approximately equally strong at L_3 and L_2 for transfers of around 2 eV, and there is apparent fluorescence intensity at comparably large energy transfers of around 10 eV at the L_3-edge. These variations are responsible for the discrepancy between the Cr PFY and absorption spectra, and with the calculations discussed below, we demonstrate that they are due to state-dependent variations in the fluorescence decay rates.

In order to refine our simulations by accounting for the variations of the fluorescence yields, we fitted the simulated to the measured Cr PFY spectrum. The best match is displayed in Figure 3a, and we find it for fluorescence yields of 2.0×10^{-3} for L_3 and 3.7×10^{-3} for L_2.

With this refinement, we find a perfect match between the measured and simulated Cr TFY spectra, as shown with the comparison in Figure 3b. This demonstrates that the dips in the TFY spectrum are solely due to X-ray optical effects as accounted for by the standard formula for fluorescence yield X-ray absorption spectroscopy and a state- or incident-photon-energy dependence of the fluorescence yield. There is no need to evoke a new process such as dark channel fluorescence yield or an additional intermolecular mechanism such as charge transfer to the solvent to explain the dips. With this, we fully confirm the theoretical analysis of TFY spectra of free Fe^{3+} ions by de Groot.[29] A more detailed presentation of the simulations of the X-ray optical effects will be published elsewhere. Our simulations indicate that the main contributions to the X-ray optical effects are the variation of the background fluorescence, confirming the claim in ref 30, and a variation of the experimental geometry, which, in turn, mainly affects the contribution of saturation.[31] Together with the state-dependent fluorescence yield as detected here for aqueous Cr^{3+}, we can, in general, explain the dips in the TFY of 3d transition-metal ions and complexes in solution. In particular, some approximate trends can be readily explained.[29,30] The strength of the dips in the TFY spectra of 3d transition-metal ions in water decreases for increasing Z[21] and with increasing fluorescence yield of the solute compared to the fluorescence yield of O in water. Furthermore, for a given 3d transition-metal ion, the strength of the dip decreases when going from water to alcohols as solvent due to the increased absorption of the additional C atoms in the alcohol molecules. Finally, no dips were observed in several solvated species,[37,38] as can be explained by their low concentration compared to the concentrations used here and in the studies where dips were reported.[21−24,27,28]

The questions remain as to what is the origin of the state-dependent fluorescence decay rate in aqueous Cr^{3+} and whether it can be related to interactions between the metal ion and the solvent molecules in general or to a charge transfer to the solvent in particular. In order to answer these questions, we performed

dx.doi.org/10.1021/jz301486u | J. Phys. Chem. Lett. 2012, 3, 3448−3453

two types of calculations that mainly differ in the way that the intermolecular interactions are treated. The calculated Cr L-edge X-ray absorption and PFY spectra are displayed in Figure 4.

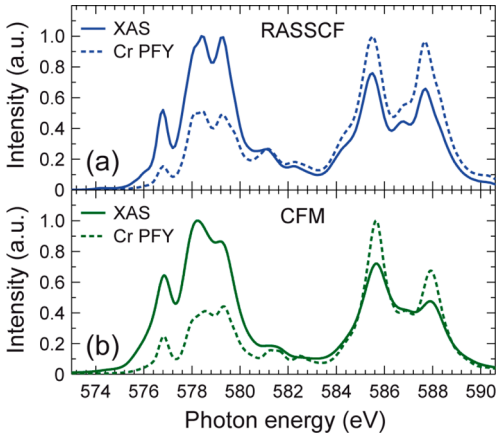

Figure 4. Theoretical X-ray absorption spectra (XAS, solid lines) and Cr PFY spectra (dashed lines) as calculated within the RASPT2 (a) and CFM (b) approaches (see text). All spectra are normalized to 1 at the maximum.

The ab initio RASPT2 calculations of a $[Cr(H_2O)_6]^{3+}$ complex are based on a molecular orbital approach, including the interactions of the Cr^{3+} ion with the water ligands with an accurate explicit treatment of both electrostatic and covalent intermolecular interactions. The semiempirical CFM calculations are based on localized atomic orbitals,[39] and the ligand environment is approximated by a crystal field using the ligand field parameter $10Dq$ and by scaling of the Slater integrals without explicit inclusion of intermolecular interactions. The calculated X-ray absorption and PFY spectra in Figure 4 agree well with the corresponding measured spectra in Figure 1. This confirms the well-known fact that L-edge absorption features in the spectra of 3d transition-metal ions are dominated by allowed transitions to the atomic multiplet states of the open-shell $2p^53d^n$ configuration ($n = 4$ for aqueous Cr^{3+}). Note that this is the only core-excited configuration included in our calculations, and, in particular, no configurations where charge has transferred to the ligands need to be included to reach agreement with experiment. For sure, electrons do not transfer during the core−hole lifetime in aqueous Cr^{3+}. Furthermore, the calculations reproduce the measured deviation of the PFY spectrum compared to the absorption spectrum. In both calculations for the PFY spectra, the fluorescence yields were approximated to be proportional to the fluorescence decay rates (see the Supporting Information). This confirms that inclusion of state-to-state variations in the fluorescence decay rates is sufficient to explain the difference between the PFY and absorption spectra.

It is important not to confuse charge-transfer processes as discussed here with covalent interactions, which are also often described in terms of charge transfer. Our RASPT2 calculations can be used to infer details of the intermolecular interactions in the $[Cr(H_2O)_6]^{3+}$ complex. They show that covalent interactions between Cr^{3+} and H_2O are definitely present. However, the mixing of Cr 3d orbitals with the water lone pair $1b_2$ and the $3a_1$ orbitals is weak, and bonding is mostly ionic. As the Cr 3d orbitals are only partially occupied, the weak covalent interaction is of ligand-to-metal charge-transfer type, resulting in a small increase of 3d orbital occupancy. Charge is thus partially transferred in terms of orbital mixing in the opposite direction compared to what had been evoked by Aziz et al.[21] In a ligated metal ion, charge transfer in the framework of covalent bonding is always referenced to the metal ion without ligands. This is different from the transient charge-transfer process in core-excited states as postulated by Aziz et al.

Finally, both our theoretical approaches correctly describe the essential local atomic electron repulsion and spin−orbit interactions in the core-excited states. A large number of states are present as a result of the many possible determinants of the $2p^53d^4$ configuration in Cr^{3+}. These determinants are mixed due to the inter- and intra-atomic interactions, including spin−orbit coupling. It is thus no surprise that the core-excited states, which are composed of determinants with different symmetry and spin, can overlap differently with the valence-excited RIXS final states. The state-dependent fluorescence rate is thus a local atomic effect[29] and simply results from the large number of states of the Cr^{3+} $2p^53d^4$ configuration. This is of utmost importance as it shows that one cannot infer from a variation of the fluorescence yield a delocalization of the excited electron or even upon orbital mixing or hybridization, as recently insinuated.[27,28,40,41]

In conclusion, we present a consistent set of experimental and theoretical data for a transition-metal ion in solution that allows us to disentangle local atomic effects, intermolecular interactions, and X-ray optical effects. We show, in particular, that the dips in the Cr L-edge TFY spectrum of aqueous Cr^{3+} cannot be interpreted in terms of charge transfer to solvent effects. We find no evidence for the asserted dark channel fluorescence. Instead, the TFY spectra are dominated by straightforward X-ray optical and local atomic effects. Mainly, these are a variation of the solvent or background fluorescence intensity and of saturation. In addition, we find a strong state- or incident-photon-energy dependence of the fluorescence yield due to a state dependence of the fluorescence decay rates. This local atomic effect in turn is a natural consequence of the large number of core-excited states at the Cr L-edges as a result of the partially filled 3d shell. We address the bonding in the $[Cr(H_2O)_6]^{3+}$ complex, and besides ionic interactions, we find a covalent contribution of ligand-to-metal charge-transfer character. On the basis of our results, we conclude that TFY spectra of 3d transition-metal ions and complexes in solution cannot be, in general, interpreted in terms of charge transfer to solvent effects.

EXPERIMENTAL SECTION

The samples consisted of aqueous solutions of $CrCl_3$ with a concentration of 1 mol/L. The solutions were prepared at least 1 day before measurement to ensure known speciation of mostly hexacoordinated Cr^{3+}. All spectra were measured at room temperature. Careful analysis of transmission-mode spectra of a solution of various ages with supposedly different speciation showed no noticeable difference. Speciation can hence be neglected for the discussed effects. The experimental transmission-mode spectrum was measured on a thin film of the sample of approximately 1 μm thickness sandwiched between two X-ray transparent windows in the setup described in ref 42 at beamline PM3 at the synchrotron radiation facility BESSYII. Both the TFY and the PFY spectra and the RIXS plane were measured on a liquid jet in vacuum (the detailed description of the setup will be published separately by Kunnus et al.) at beamlines U41 and U49 at BESSYII. The Cr RIXS plane and the Cr and O PFY spectra were measured with a Rowland-type RIXS spectrometer by detecting photons arising from fluorescence at the Cr L- and O K-edges under an angle of 90° with respect to the propagation direction of the incident radiation. The polarization of the incident radiation was linear and

dx.doi.org/10.1021/jz301486u | J. Phys. Chem. Lett. 2012, 3, 3448−3453

parallel to the detection direction of the fluorescence (in the horizontal scattering plane). Polarization effects were shown to have minor influences (Kurian et al., unpublished results). TFY spectra were measured by detecting the total fluorescence from the sample with a GaAsP diode (Hamamatsu model G-112704).

THEORETICAL CALCULATIONS

The simulations are based on the well-known formula for fluorescence-detected X-ray absorption spectroscopy, and we used its implementation from Eisebitt et al.,[31] which we modified to account for two fluorescing centers. This formula is used here to simulate all effects that one could call X-ray optical effects, such as a variation of the relative absorption strength when the solute absorption edge is scanned, self-absorption, or saturation. We assume fluorescence to arise from two species only, Cr and O, labeled 1 and 2, respectively, and the TFY spectrum being the sum of the Cr (I_{PFY1}) and O (I_{PFY2}) PFY spectra.

$$I_{TFY}(E_{in}) = I_{PFY1}(E_{in}) + I_{PFY2}(E_{in})$$

$$I_{PFY1}(E_{in}) \propto \int \frac{f_1(E_{in})\mu_1(E_{in})\Phi_1(E_{in}, E_{out1})}{\mu_1(E_{in}) + \mu_2(E_{in}) + \mu_{b1}(E_{in}) + \mu_{b2}(E_{in}) + g[\mu_1(E_{out1}) + \mu_2(E_{out1}) + \mu_{b1}(E_{out1}) + \mu_{b2}(E_{out1})]} dE_{out1}$$

$$I_{PFY2}(E_{in}) \propto \int \frac{f_2(E_{in})\mu_2(E_{in})\Phi_2(E_{in}, E_{out2})}{\mu_1(E_{in}) + \mu_2(E_{in}) + \mu_{b1}(E_{in}) + \mu_{b2}(E_{in}) + g[\mu_1(E_{out2}) + \mu_2(E_{out2}) + \mu_{b1}(E_{out2}) + \mu_{b2}(E_{out2})]} dE_{out2}$$

with E_{in} as the incident photon energy, E_{out} as the emitted photon energy, f as the fluorescence yield, μ as the linear absorption coefficient (subscript Xb refers to background absorption of respective species due to states that do not given detectable fluorescence), Φ as the area-normalized RIXS map, and g as the geometry factor, $g \equiv \sin(\alpha)/\sin(\beta)$ (α is the grazing incidence angle, and β is the grazing outgoing angle).

As experimental inputs for the simulations, we used experimental X-ray absorption cross sections measured in transmission mode for the reported sample solution at the Cr L-edge [$\mu_1(E_{in})$, shown in Figure 1a] and at the O K-edge [$\mu_2(E_{in})$, not shown]. To describe the spectral distribution of the Cr L-edge emission, the experimental RIXS map shown in Figure 2a was used [$\Phi_1(E_{in},E_{out1})$; RIXS spectra at different incident photon energies were normalized to unit area]. To describe the O K-emission [$\Phi_2(E_{in},E_{out2})$], an experimental off-resonance X-ray emission spectrum was used (not shown). The sample thickness for the O K-edge transmission spectrum was well below 1 μm in order to avoid saturation effects. For the geometry of the simulated TFY spectrum, we assumed that the diode detects fluorescence under an angle of 45 ± 30°, corresponding approximately to the experimental implementation.

The restricted active space (RASSCF) calculations followed closely the scheme developed for Ni^{2+}(aq) (Josefsson et al., unpublished results). The explicit inclusion of static electron correlation through multiconfigurational wave functions is highly suitable for the calculation of L-edge X-ray spectra. Dynamical correlation was added in a perturbative treatment (RASPT2). A minimal active space of Cr2p(RAS1=3, containing at most one hole) and Cr3d(RAS2=5) was employed. Scalar relativistic RASPT2 calculations for all resulting $2p^63d^3/2p^53d^4$ (doublet, quartet) and $2p^53d^4$ sextet states were performed on an optimized $[Cr(H_2O)_6]^{3+}$ complex (CASPT2/TZVP: Cr−O = 2.003 Å). The spin−orbit matrix elements were computed in the state-interaction framework over a basis of state-averaged RASSCF wave functions in D_{2h} symmetry. The X-ray and RIXS spectra from the high-spin ground state were calculated with the resulting complex electronic states.

For the CFM calculations,[39] we used $10Dq$ = 2 eV and a 20% reduction of the Slater integrals. The same broadening scheme was used for all calculations, 0.3 and 0.6 eV Lorentzian broadening at the L_3- and L_2-edges, respectively, and 0.3 eV Gaussian broadening (all values in fwhm) to account for the bandwidth of the incident radiation.

ASSOCIATED CONTENT

Supporting Information

Supporting text. This material is available free of charge via the Internet at http://pubs.acs.org.

AUTHOR INFORMATION

Corresponding Author

*E-mail: wernet@helmholtz-berlin.de. Phone+49 30 806213448. Fax: +49 30 806212114.

Author Contributions

The manuscript was written through contributions of all authors. All authors have given approval to the final version of the manuscript.

Funding

M.O. aknowledges support from the Swedish Research Council, Carl Tryggers Foundation, and Magnus Bergvall Foundation.

Notes

The authors declare no competing financial interest.

ACKNOWLEDGMENTS

We gratefully acknowledge support by the staff of the Helmholtz-Zentrum Berlin for support during the BESSYII beam times. We cordially thank Christian Weniger for support of the transmission measurements.

REFERENCES

(1) Stöhr, J. *NEXAFS Spectroscopy*; Springer-Verlag: Berlin, Germany, 1992.

(2) Khalil, M.; Marcus, M. A.; Smeigh, A. L.; McCusker, J. K.; Chong, H. H. W.; Schoenlein, R. W. Picosecond X-ray Absorption Spectroscopy of a Photoinduced Iron(II) Spin Crossover Reaction in Solution. *J. Phys. Chem. A* **2006**, *110*, 38−44.

(3) Bressler, C.; Milne, C.; Pham, V.-T.; ElNahhas, A.; van der Veen, R. M.; Gawelda, W.; Johnson, S.; Beaud, P.; Grolimund, D.; Kaiser, M.; et al. Femtosecond XANES Study of the Light-Induced Spin Crossover Dynamics in an Iron(II) Complex. *Science* **2009**, *323*, 489−492.

(4) Nozawa, S.; Sato, T.; Chollet, M.; Ichiyanagi, K.; Tomita, A.; Fujii, H.; Adachi, S.-I.; Koshihara, S.-Y. Direct Probing of Spin State Dynamics Coupled with Electronic and Structural Modifications by Picosecond Time-Resolved XAFS. *J. Am. Chem. Soc.* **2010**, *132*, 61−63.

(5) Vankó, G.; Glatzel, P.; Pham, V.-T.; Abela, R.; Grolimund, D.; Borca, C. N.; Johnson, S. L.; Milne, C. J.; Bressler, C. Picosecond Time-

Resolved X-ray Emission Spectroscopy: Ultrafast Spin-State Determination in an Iron Complex. *Angew. Chem., Int. Ed.* **2010**, *49*, 5910−5912.
(6) Huse, N.; Cho, H.; Hong, K.; Jamula, L.; de Groot, F. M.; Kim, T. K.; McCusker, J. K.; Schoenlein, R. W. Femtosecond Soft X-ray Spectroscopy of Solvated Transition-Metal Complexes: Deciphering the Interplay of Electronic and Structural Dynamics. *J. Phys. Chem. Lett.* **2011**, *2*, 880−884.
(7) Chen, L. X.; Jager, W. J. H.; Jennings, G.; Gosztola, D. J.; Munkholm, A.; Hessler, J. P. Capturing a Photoexcited Molecular Structure Through Time-Domain X-ray Absorption Fine Structure. *Science* **2001**, *292*, 262−264.
(8) Wernet, Ph.; Gavrila, G.; Godehusen, K.; Weniger, C.; Nibbering, E.; Elsaesser, T.; Eberhardt, W. Ultrafast Temperature Jump in Liquid Water Studied by a Novel Infrared Pump−X-ray Probe Technique. *Appl. Phys. A: Mater. Sci. Process.* **2008**, *92*, 511−516.
(9) Huse, N.; Wen, H.; Nordlund, D.; Szilagyi, E.; Daranciang, D.; Miller, T. A.; Nilsson, A.; Schoenlein, R. W.; Lindenberg, A. M. Probing the Hydrogen-Bond Network of Water via Time-Resolved Soft X-ray Spectroscopy. *Phys. Chem. Chem. Phys.* **2009**, *11*, 3951−3957.
(10) Elles, C. G.; Shkrob, I. A.; Crowell, R. A.; Arms, D. A.; Landahl, E. C. Transient X-ray Absorption Spectroscopy of Hydrated Halogen Atom. *J. Chem. Phys.* **2008**, *128*, 061102/1−061102/4.
(11) Wernet, Ph. Electronic Structure in Real Time: Mapping Valence Electron Rearrangements During Chemical Reactions. *Phys. Chem. Chem. Phys.* **2011**, *13*, 16941−16954.
(12) Björneholm, O.; Nilsson, A.; Sandell, A.; Hernnäs, B.; Martensson, N. Determination of Time Scales for Charge-Transfer Screening in Physisorbed Molecules. *Phys. Rev. Lett.* **1992**, *68*, 1892−1895.
(13) Karis, O.; Nilsson, A.; Weinelt, M.; Wiell, T.; Puglia, C.; Wassdahl, N.; Mårtensson, N.; Samant, M.; Stöhr, J. One-Step and Two-Step Description of Deexcitation Processes in Weakly Interacting Systems. *Phys. Rev. Lett.* **1996**, *76*, 1380−1383.
(14) Keller, C.; Stichler, M.; Comelli, G.; Esch, F.; Lizzit, S.; Wurth, W.; Menzel, D. Ultrafast Charge Transfer Times of Chemisorbed Species from Auger Resonant Raman Studies. *Phys. Rev. Lett.* **1998**, *80*, 1774−1777.
(15) Wurth, W.; Menzel, D. Ultrafast Electron Dynamics at Surfaces Probed by Resonant Auger Spectroscopy. *Chem. Phys.* **2000**, *251*, 141−149.
(16) Schnadt, J.; Brühwiler, P. A.; Patthey, L.; O'Shea, J. N.; Södergren, S.; Odelius, M.; Ahuja, R.; Karis, O.; Bässler, M.; Persson, P.; et al. Experimental Evidence for Sub-3-fs Charge Transfer from an Aromatic Adsorbate to a Semiconductor. *Nature* **2002**, *418*, 620−623.
(17) Brühwiler, P.; Karis, O.; Mårtensson, N. Charge-Transfer Dynamics Studied Using Resonant Core Spectroscopies. *Rev. Mod. Phys.* **2002**, *74*, 703−740.
(18) Föhlisch, A.; Feulner, P.; Hennies, F.; Fink, A.; Menzel, D.; Sanchez-Portal, D.; Echenique, P. M.; Wurth, W. Direct Observation of Electron Dynamics in the Attosecond Domain. *Nature* **2005**, *436*, 373−376.
(19) Nordlund, D.; Ogasawara, H.; Bluhm, H.; Takahashi, O.; Odelius, M.; Nagasono, M.; Pettersson, L. G. M.; Nilsson, A. Probing the Electron Delocalization in Liquid Water and Ice at Attosecond Time Scales. *Phys. Rev. Lett.* **2007**, *99*, 217406/1−217406/4.
(20) Aziz, E. F.; Ottosson, N.; Faubel, M.; Hertel, I. V.; Winter, B. Interaction Between Liquid Water and Hydroxide Revealed by Core−Hole De-excitation. *Nature* **2008**, *455*, 89−91.
(21) Aziz, E. F.; Rittmann-Frank, M. H.; Lange, K. M.; Bonhommeau, S.; Chergui, M. Charge Transfer to Solvent Identified Using Dark Channel Fluorescence-Yield L-Edge Spectroscopy. *Nat. Chem.* **2010**, *2*, 853−857.
(22) Bauer, M.; Stalinski, T.; Aziz, E. F. Insights into the Induced Ultrafast Electron Delocalization in $Fe(CO)_5$ Using Dark Channel Fluorescence Yield X-ray Spectroscopy. *Chem. Phys. Chem.* **2011**, *12*, 2088−2091.
(23) Lange, K.; Kothe, A.; Aziz, E. F. Chemistry in Solution: Recent Techniques and Applications Using Soft X-ray Spectroscopy. *Phys. Chem. Chem. Phys.* **2012**, *14*, 5331−5338.
(24) Aziz, E. F. X-ray Spectroscopies Revealing the Structure and Dynamics of Metalloprotein Active Centers. *J. Phys. Chem. Lett.* **2011**, *2*, 320−326.
(25) Nilsson, A. X-ray Spectroscopy: Transferring Electrons to Water. *Nat. Chem.* **2010**, *2*, 800−802.
(26) Näslund, L.-Å.; Cavalleri, M.; Ogasawara, H.; Wernet, Ph.; Edwards, D. C.; Sandstroem, M.; Myneni, S.; Nilsson, A.; Pettersson, L. G. M. Direct Evidence of Orbital Mixing Between Water and Solvated Transition Metal Ions: An Oxygen 1s XAS and DFT Study of Aqueous Systems. *J. Phys. Chem. A* **2003**, *107*, 6869−6876.
(27) Seidel, R.; Ghadimi, S.; Lange, K. M.; Bonhommeau, S.; Soldatov, M. A.; Golnak, R.; Kothe, A.; Könnecke, R.; Soldatov, A.; Thürmer, S.; et al. F. Origin of Dark-Channel X-ray Fluorescence from Transition-Metal Ions in Water. *J. Am. Chem. Soc.* **2012**, *134*, 1600−1605.
(28) Soldatov, M. A.; Lange, K. M.; Gotz, M. D.; Engel, N.; Golnak, R.; Kothe, A.; Aziz, E. F. On the Origin of Dips in Total Fluorescence Yield X-ray Absorption Spectra: Partial and Inverse Partial Fluorescence Yield at the L-Edge of Cobalt Aqueous Solution. *Chem. Phys. Lett.* **2012**, *546*, 164−167.
(29) de Groot, F. M. F. Dips and Peaks in Fluorescence Yield X-ray Absorption Are Due To State-Dependent Decay. *Nat. Chem.* **2012**, *4*, 766−767.
(30) Regier, T. Z.; Achkar, A. J.; Peak, D.; Tse, J. S.; Hawthorn, D. G. Dark Channel Fluorescence Observations Result from Concentration Effects Rather than Solvent−Solute Charge Transfer. *Nat. Chem.* **2012**, *4*, 765−766.
(31) Eisebitt, S.; Böske, T.; Rubensson, J.-E.; Eberhardt, W. Determination of Absorption Coefficients for Concentrated Samples by Fluorescence Detection. *Phys. Rev. B* **1993**, *47*, 14103−14109.
(32) Achkar, A. J.; Regier, T. Z.; Wadati, H.; Kim, Y.-J.; Zhang, H.; Hawthorn, D. G. Bulk Sensitive X-ray Absorption Spectroscopy Free of Self-Absorption Effects. *Phys. Rev. B* **2011**, *83*, 081106(R)/1−081106(R)/4.
(33) de Groot, F. M. F. Fluorescence Yield Detection: Why It Does Not Measure the X-Ray Absorption Cross Section. *Solid State Commun.* **1994**, *92*, 991−995.
(34) Krause, O. Atomic Radiative and Radiationless Yields for K and L Shells. *J. Phys. Chem. Ref. Data* **1979**, *8*, 307−328.
(35) Coster, D.; Kronig, R.; De, L. New Type of Auger Effect and Its Influence on the X-ray Spectrum. *Physica* **1935**, *2*, 13−24.
(36) Gotz, M. D.; Soldatov, M. A.; Lange, K. M.; Engel, N.; Golnak, R.; Könnecke, R.; Atak, K.; Eberhardt, W.; Aziz, E. F. Probing Coster−Kronig Transitions in Aqueous Fe^{2+} Solution Using Inverse Partial and Partial Fluorescence Yield at the L-Edge. *J. Phys. Chem. Lett.* **2012**, *3*, 1619−1623.
(37) Aziz, E. F.; Ottosson, N.; Bonhommeau, S.; Bergmann, N.; Eberhardt, W.; Chergui, M. Probing the Electronic Structure of the Hemoglobin Active Center in Physiological Solutions. *Phys. Rev. Lett.* **2009**, *102*, 068103/1−068103/4.
(38) Bergmann, N.; Bonhommeau, S.; Lange, K. M.; Greil, S. M.; Eisebitt, S.; de Groot, F. M. F.; Chergui, M.; Aziz, E. F. On the Enzymatic Activity of Catalase: An Iron L-Edge X-ray Absorption Study of the Active Centre. *Phys. Chem. Chem. Phys.* **2010**, *12*, 4827−4832.
(39) Stavitski, E.; de Groot, F. M. F. The CTM4XAS Program for EELS and XAS Spectral Shape Analysis of Transition Metal L Edges. *Micron* **2010**, *41*, 687−694.
(40) Aziz, E. F.; Lange, K. M.; Bonhommeau, S.; Chergui, M. Reply to 'Dark Channel Fluorescence...' and 'Dips and Peaks...'. *Nat. Chem.* **2012**, *4*, 767−768.
(41) Lange, K. M.; Suljoti, E.; Aziz, E. F. Resonant Inelastic X-Ray Scattering as a Probe of Molecular Structure and Electron Dynamics in Solutions. *J. Electron Spectrosc. Relat. Phenom.* **2012**, DOI: 10.1016/j.elspec.2012.09.010.
(42) Schreck, S.; Gavrila, G.; Weniger, C.; Wernet, Ph. A Sample Holder for Soft X-ray Absorption Spectroscopy of Liquids in Transmission Mode. *Rev. Sci. Instrum.* **2011**, *82*, 103101/1−103101/10.